Eur J Nucl Med Mol Imaging (2016) 43:2290–2300
DOI 10.1007/s00259-016-3448-8

ORIGINAL ARTICLE

Development of computational pregnant female and fetus models and assessment of radiation dose from positron-emitting tracers

Tianwu Xie[1] · **Habib Zaidi**[1,2,3,4]

Received: 8 April 2016 / Accepted: 16 June 2016 / Published online: 28 June 2016

Abstract
Purpose Molecular imaging using PET and hybrid (PET/CT and PET/MR) modalities nowadays plays a pivotal role in the clinical setting for diagnosis and staging, treatment response monitoring, and radiation therapy treatment planning of a wide range of oncologic malignancies. The developing embryo/fetus presents a high sensitivity to ionizing radiation. Therefore, estimation of the radiation dose delivered to the embryo/fetus and pregnant patients from PET examinations to assess potential radiation risks is highly praised.
Methods We constructed eight embryo/fetus models at various gestation periods with 25 identified tissues according to reference data recommended by the ICRP publication 89 representing the anatomy of the developing embryo/fetus. The developed embryo/fetus models were integrated into realistic anthropomorphic computational phantoms of the pregnant female and used for estimating, using Monte Carlo calculations, S-values of common positron-emitting radionuclides, organ absorbed dose, and effective dose of a number of positron-emitting labeled radiotracers.
Results The absorbed dose is nonuniformly distributed in the fetus. The absorbed dose of the kidney and liver of the 8-week-old fetus are about 47.45 % and 44.76 % higher than the average absorbed dose of the fetal total body for all investigated radiotracers. For ^{18}F-FDG, the fetal effective doses are 2.90E-02, 3.09E-02, 1.79E-02, 1.59E-02, 1.47E-02, 1.40E-02, 1.37E-02, and 1.27E-02 mSv/MBq at the 8th, 10th, 15th, 20th, 25th, 30th, 35th, and 38th weeks of gestation, respectively.
Conclusion The developed pregnant female/fetus models matching the ICRP reference data can be exploited by dedicated software packages for internal and external dose calculations. The generated S-values will be useful to produce new standardized dose estimates to pregnant patients and embryo/fetus from a variety of positron-emitting labeled radiotracers.

Keywords PET · Radiation dosimetry · Pregnant female models · Monte Carlo · Simulation

Introduction

PET makes use of positron-emitting labeled tracers to visualize and quantify in vivo biochemical processes and molecular events occurring in the human body. It has been widely adopted as an important tool for clinical diagnosis, prognosis, staging and restaging, monitoring response to treatment, and radiation therapy planning of a variety of oncologic malignancies [1]. Similar to concerns raised for the pediatric population [2, 3], radiation exposure of pregnant or potentially pregnant patients is becoming an increasingly important and concerning issue in diagnostic imaging owing to the high risks related to radiation exposure of the developing fetus. Overall,

Electronic supplementary material The online version of this article (doi:10.1007/s00259-016-3448-8) contains supplementary material, which is available to authorized users.

✉ Habib Zaidi
habib.zaidi@hcuge.ch

[1] Division of Nuclear Medicine and Molecular Imaging, Geneva University Hospital, CH-1211 Geneva, Switzerland

[2] Geneva Neuroscience Center, Geneva University, Geneva, Switzerland

[3] Department of Nuclear Medicine and Molecular Imaging, University of Groningen, University Medical Center Groningen, Groningen, Netherlands

[4] Department of Nuclear Medicine, University of Southern Denmark, DK-500 Odense, Denmark

the gestational age and the fetal absorbed dose level determine the risks associated with the risks of using ionizing radiation. During 8–15 weeks of gestation (early pregnancy), the embryo/fetus presents the highest sensitivity to ionizing radiation where radiation exposure might induce non-stochastic effects, i.e. embryonic death, growth retardation, anatomic malformation, and microcephaly at a threshold between 0.35-0.5 Gy [4]. For a fetus of 16–40 weeks, radiation exposure is associated with non-stochastic effects of growth retardation, decreased brain size, and mental retardation at a threshold of 1.5 Gy and stochastic effects of childhood cancer when fetal absorbed dose exceeds 100 mGy [5]. The fetal nervous system exhibits a long period of sensitivity to ionizing radiation during the whole gestation period and its development is known to be affected by radiation exposure above 50 cGy [6]. In this context, accurate estimation of the radiation dose plays an essential role in risk analysis during the decision making process when attempting to balance the benefits of radiologic imaging for diseased pregnant patients with the radiation risks to the developing fetus.

Several computational models of pregnant women and fetus have been developed and incorporated within Monte Carlo calculations for assessing fetal radiation dose in radiologic imaging procedures [7]. Stabin et al. [8] and Russell et al. [9] constructed the first complete set of pregnant female models using simple mathematical surface equations to estimate the fetal dose at early pregnancy and at the 3rd trimester for a large number of radiopharmaceuticals. The developed mathematical pregnant female models have been integrated in the MIRDOSE and OLINDA/EXM personal computer software packages for internal dose assessment. They were used by Zanotti-Fregonara et al. [10–12] and Takalkar et al. [13] to estimate the fetal absorbed dose at various gestation periods from ^{18}F-FDG examinations of pregnant patients. However, mathematical models are commonly used for estimating radiation dose to the embryo/fetus in published literatures [9, 14, 15] while the organ-level radiation dose of the developing fetus is rarely reported. With the development of anthropomorphic computational phantoms and the continuously increasing number of PET radiotracers targeting various molecular targets, the assessment of the fetal radiation dose from common positron-emitting radiotracers using new generation pregnant female phantoms providing detailed anatomic description of fetal internal organs is needed.

In this work, we develop a complete set of embryo/fetus models at the 8th, 10th, 15th, 20th, 25th, 30th, 35th, and 38th weeks of gestation with 25 identified tissues according to the reference fetal anatomic data recommended by the ICRP [16]. The developed fetus models were integrated within the anthropomorphic pregnant female phantoms to run Monte Carlo-based particle transport simulations of common positron-emitting radionuclides. S-values, absorbed and effective doses to the pregnant female and fetus from positron-emitting radionuclides and commonly used positron-emitting labeled radiotracers were calculated. The produced radiation dosimetry database provides a systematic estimate of fetal organ-level radiation dose from positron-emitting labeled radiopharmaceuticals, whereas the calculated S-values can be used for the assessment of the radiation dose to the fetus from new PET-based molecular imaging probes.

The pregnant female phantom series of the Rensselaer Polytechnic Institute (RPI) (12th, 24th, and 36th weeks of gestation) [17], the Fetal and Mother Numerical Models (FEMONUM) developed by Telecom ParisTech (8th, 10th, 26th, 30th, and 35th weeks of gestation) [18], the Katja phantom [19] (24th week of gestation), as well as the voxel newborn model [20] of Helmholtz Zentrum München were used in this work to construct new series of fetal/pregnant female models [21]. The FEMONUM utero-fetus models at the 8th and 10th weeks of gestation were constructed based on medical images acquired using 3-D ultrasound imaging while the FEMONUM utero-fetus models of the 26th, 30th, and 35th weeks of gestation were constructed using 3-D magnetic resonance imaging (MRI) data. The RPI pregnancy phantoms were constructed based on CT images of a pregnant female (7th month of gestation) and the VIP-Man model. The Katja fetus model was constructed based on abdominal MRI images of a pregnant patient at 24th week of pregnancy, while the newborn baby model of Helmholtz Zentrum München was constructed from CT scans of a donated baby body.

Materials and methods

Development of pregnant female phantom series

In this work, the voxel-based Katja phantom and newborn phantom of Helmholtz Zentrum München were transformed to corresponding non-uniform rational basis spline (NURBS) surface representation models using an in-house developed C++ code and the Rhinoceros™ package to develop a new set of fetal/pregnant female models. The body contour and maternal internal organs of RPI phantoms were adapted. FEMONUM phantoms were used for defining the placenta, umbilical cord, vesicle Vitelline, uterine wall, amniotic fluid, and fetal body contours of the constructed models at the 8th and 10th weeks of gestation. The bone marrow and skeleton of the fetus phantoms were scaled from the fetal skeleton of the RPI phantom at 9 months of gestation to match the reference organ mass of the ICRP [16]. The fetal organs, including adrenal, pancreas, spleen, and thymus, were scaled from the voxel newborn model of Helmholtz Zentrum München to match the reference organ mass of ICRP [16]. For the lung, brain, heart, eyes, stomach, gall bladder, the organs of the fetus model at 8–20 weeks of gestation were scaled from the Katja model. The organs of the fetus model at 25–35 weeks of

gestation were scaled from FEMONUM models, whereas the organs of the fetus model at 38 weeks of gestation were scaled from organs of the voxel newborn model. A pipe model along the fetal spine was constructed to represent the spinal cord. The fetal liver and kidney models at 8–30 weeks of gestation and 35–38 weeks of gestation were scaled from the Katja model and the newborn model, respectively. A description of the sources of the constructed maternal body and fetal organ masses is listed in Supplemental Table S1. The target masses of fetal organs at different gestation periods were obtained from the ICRP reference dataset. The maternal breast, contour of maternal abdomen, maternal bladder, maternal small intestine (SI), and large intestine (LI) at different gestation periods were manually adjusted using the Rhinoceros™ package. A total of 35 maternal tissues and 25 fetal regions were included in the surface representing pregnant female phantom series constructed in this work. Figure 1 shows 3D visualization of the front views and side views of the developed computational pregnant phantoms at various gestation periods. Figure 2 shows a 3D visualization of the developed embryo/fetus models with the placenta and umbilical cord.

Radiation dose calculations

The developed computational pregnant female phantoms were voxelized using the *Binvox* package [22] and imported to the MCNPX code [23] for radiation transport simulations. S-values of uniformly distributed positron-emitting sources in all identified maternal and fetal tissues were calculated. Absorbed dose and effective dose delivered to fetal and maternal body organs from a number of PET radiotracers, including ^{11}C-Acetate, ^{11}C- and ^{18}F-Amino acids, ^{11}C-Methionine, ^{11}C- and ^{18}F-Brain receptor substances, ^{11}C (Realistic maximum model), [Methyl-^{11}C]-Thymidine, ^{11}C-Thymidine, ^{11}C-1-(3,4-dimethoxyphenethyl)-4-(3-phenylprophyl)piperazine (^{11}C-SA4503), ^{11}C-8-dicyclopropylmethyl-1-methyl-3-propylxanthine (^{11}C-MPDX), ^{11}C-(E)-8-(3,4,5-trimethoxystyryl)-1,3,7-trimethylxanthine (^{11}C-TMSX), 4-^{11}C-methylphenyl-1,4-diazabicyclo[3.2.2.]nonane-4-carboxylate (^{11}C-CHIBA-1001), ^{11}C-4'-thiothymidine (^{11}C-4DST), ^{15}O-water, 2-[^{18}F]Fluoro-2-deoxy-D-glucose (^{18}F-FDG), 6-[^{18}F]Fluoro-L-dopa (^{18}F-L-dopa), 4-borono-2-^{18}F-fluoro-L-phenylalanine (^{18}F-FBPA), 6-[^{18}F]Fluorodopamine (^{18}F-FDOPA), ^{68}Ga-ethylenediaminetetraacetic acid (^{68}Ga-EDTA), and ^{68}Ga-[1,4,7,10-Tetraazacyclododecane-1,4,7,10-tetraacetic acid]-1-Nal3-octreotide (^{68}Ga-DOTANOC) were calculated based on biokinetic data reported in ICRP publications [24, 25] and other published literature [26, 27]. The Medical Internal Radiation Dose (MIRD) formalism [28], ICRP 103 recommendations [29] and the estimated fetal mean residence times (MRTs) from our previous work [15] were employed to calculate S-values, radiation absorbed dose and effective dose in the new series of fetal/pregnant female phantoms. For each radiotracer, maternal organs are classified into two types: organs of type I, which include organs with MRTs given in the ICRP reports or in the literature, and organs of

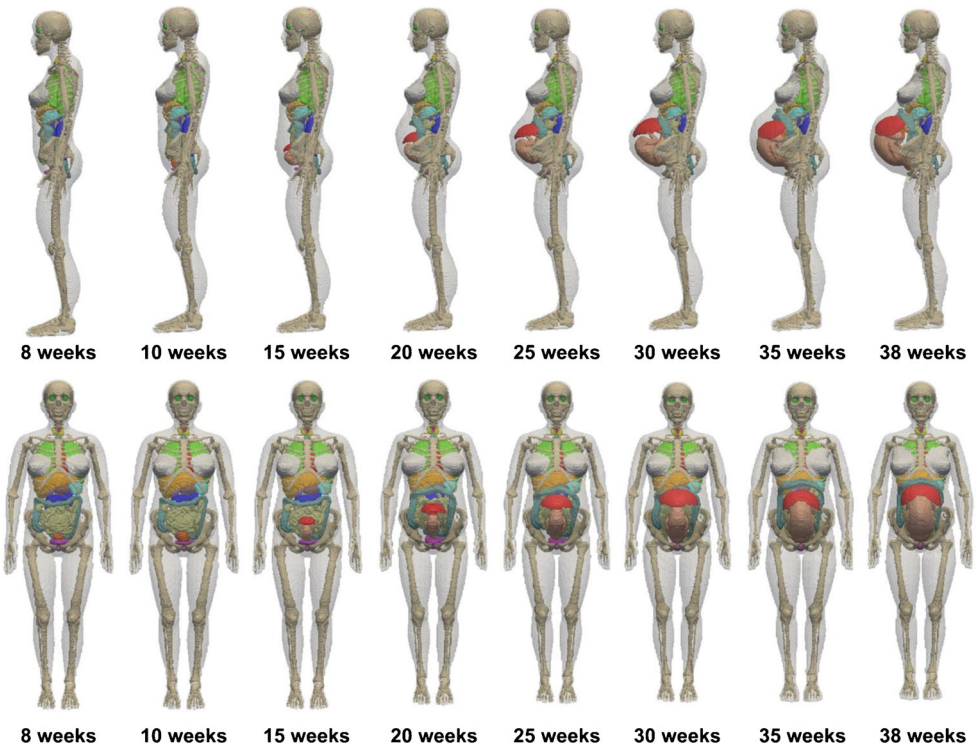

Fig. 1 3D visualization of the developed computational pregnant female phantoms at different gestations showing (**a**) side views and (**b**) front views, respectively. The uterine was set transparent to exhibit the fetus

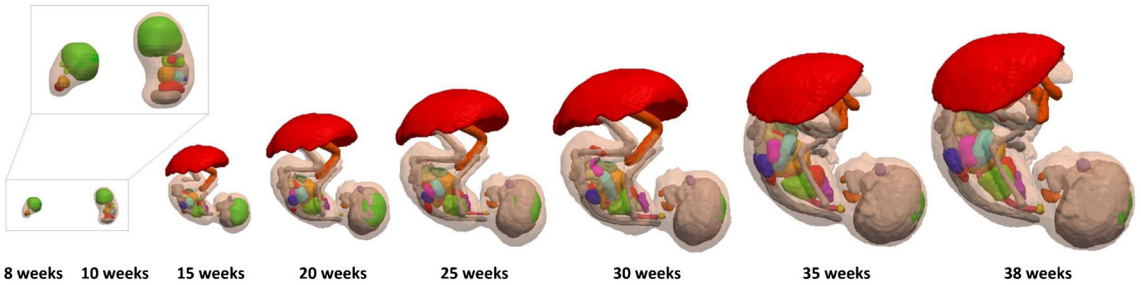

Fig. 2 3D visualization of the fetal phantoms at different gestation periods

type II that encompass all the other organs. For organs of type I of the maternal body, the MRTs were calculated as:

$$\mathrm{MRT}_{\mathrm{maternal}}^{\mathrm{Type\ I}} = \mathrm{MRT}_{\mathrm{R}}^{\mathrm{Type\ I}} \times \frac{\mathrm{Volume}_{\mathrm{maternal}}^{\mathrm{TB}}}{\mathrm{Volume}_{\mathrm{maternal}}^{\mathrm{TB}} + \mathrm{Volume}_{\mathrm{fetal}}^{\mathrm{TB}}},$$

For maternal organs of type II, the MRTs were calculated as:

$$\mathrm{MRT}_{\mathrm{maternal}}^{\mathrm{Type\ II}} = \left(\mathrm{MRT}_{\mathrm{R}}^{\mathrm{Sum}} - \sum \mathrm{MRT}_{\mathrm{R}}^{\mathrm{Type\ I}}\right) \times \left(\frac{\mathrm{Volume}_{\mathrm{maternal}}^{\mathrm{TB}}}{\mathrm{Volume}_{\mathrm{maternal}}^{\mathrm{TB}} + \mathrm{Volume}_{\mathrm{fetal}}^{\mathrm{TB}}}\right) \times \left(\frac{\mathrm{Volume}_{\mathrm{maternal}}^{\mathrm{Type\ II}}}{\mathrm{Volume}_{\mathrm{maternal}}^{\mathrm{TB}} - \sum \mathrm{Volume}_{\mathrm{maternal}}^{\mathrm{Type\ I}}}\right).$$

For fetal organs, the MRTs are given by:

$$\mathrm{MRT}_{\mathrm{fetus}}^{\mathrm{organ}} = \left(\mathrm{MRT}_{\mathrm{R}}^{\mathrm{Sum}} \times \frac{\mathrm{Volume}_{\mathrm{fetal}}^{\mathrm{TB}}}{\mathrm{Volume}_{\mathrm{maternal}}^{\mathrm{TB}} + \mathrm{Volume}_{\mathrm{fetal}}^{\mathrm{TB}}}\right) \times \frac{\mathrm{Volume}_{\mathrm{fetus}}^{\mathrm{organ}}}{\mathrm{Volume}_{\mathrm{fetal}}^{\mathrm{TB}}},$$

where MRT_{R}^{Sum} refers to the sum of reported mean residence times of certain radiotracers in the adult body. The developing embryo/fetus may uptake the injected compounds from maternal blood. In accordance with Benveniste et al. [30], which suggested similar uptake values for fetal and maternal activity for FDG, an equal average activity concentration in maternal and fetal tissues was assumed for all investigated radiotracers [15].

Fetal dose from ^{18}F-FDG in clinical scans

^{18}F-FDG is the workhorse of PET scanning and the most commonly used PET tracer in oncology. The diagnosis of cancer using FDG-PET during pregnancy is relatively rare. However, few studies [12, 13] reported on a series of eleven patients at 5–30 weeks of pregnancy that underwent ^{18}F-FDG scans for diagnostic workup for cancer. In both studies, FDG time-integrated activity coefficients of the fetus were calculated based on PET images and combined with four anthropomorphic phantoms of pregnant women at early pregnancy, first, second, and third trimesters, respectively, to calculate fetal doses. In this work, we recalculated the fetal dose in the eleven reported cases based on the time-integrated activity coefficients in the fetal bodies provided reported in the above referenced works [12, 13] and the new series of anthropomorphic pregnant female phantoms at eight gestation periods. The ICRP biokinetic data were used to determine the time-integrated activity coefficients of FDG in maternal organs.

Results

Developed pregnant female phantom series

Organ and tissue masses of the developed computational pregnant female phantoms are listed in Supplemental Table S2. The fetal skin was generated by assigning a skin tag to the outermost voxel layer of the fetal body contour. Percent differences between organ masses of the developed series of pregnant female phantoms and ICRP 89 reference values are also shown. The total body masses of most fetus models were matched to ICRP reference data to within 0.2 % while the fetus model at 8 weeks of pregnancy has a total mass 12.98 % higher than the reference value. All maternal tissues were matched to reference masses within 1 %, except the breasts, eyeballs, and eye lens. For fetus models above 15 weeks of gestation, all fetal tissues were matched to ICRP reference masses to within 0.3 %. For fetus models at early pregnancy (8th week and 10th week), the fetal total body weight was set at its reference value and, consequently, it was not possible to accommodate a larger mass for bone marrow, thyroid, kidneys, adrenals, and pancreas in the fetus models without concomitant expansion of the fetal body contour.

S-values for positron-emitting radionuclides

S-values of 69 target regions from nine positron-emitting radionuclides (C-11, N-13, O-15, F-18, Cu-64, Ga-68, Rb-82, Y-86, and I-124) calculated for the constructed female

phantom series are provided in the Supplemental Table S3. Figure 3 compares the self-absorbed S-values from F-18 to representative targeted fetal regions. At 8 weeks of pregnancy, the fetal thyroid presents the highest self-absorbed S-values from F-18 (3.11 mGy/MBq.s), while the fetal brain presents the lowest self-absorbed S-value from F-18 (1.08E-02 mGy/MBq.s).

Figure 4 shows the self-absorbed S-values for maternal total body and fetal total body. The self-absorbed S-values of the maternal total body are almost constant at different gestation periods while self-absorbed S-values of the fetal total body decrease with gestational age. The self-absorbed S-values of fetal organs decrease with gestational age. For the considered positron-emitting radionuclides, the average relative difference of fetal self-absorbed S-values per kg difference in fetal weight (%/kg) between the 8th and 38th week of pregnancy is −28.3 %/kg. Figure 5 shows the cross-absorbed S-values of F-18 and Ga-68 of representative fetal organs from the maternal total body and maternal urinary bladder. For F-18, the cross-absorbed S-values for maternal total body irradiating fetal total body and organs are mostly contributed by the two annihilation photons and follow a linear relationship with gestational age.

Absorbed and effective doses

Absorbed doses of 35 maternal organs and 25 fetal organs from 21 common positron-emitting radiotracers were evaluated (Supplemental Tables S4-S5). Figure 6 shows the absorbed dose from ^{18}F-FDG to representative fetal tissues and maternal organs. For most targeted maternal regions, except the bladder wall, the absorbed dose from radiotracers decreases slightly with the gestational age. The absorbed dose is non-uniformly distributed in the fetus. The absorbed dose of the fetal kidney and liver of the 8-week-old fetus are about 47.45 % and 44.76 % higher than the average absorbed dose of the fetal total body for the 21 evaluated radiotracers. The fetal kidney and liver receive the highest dose from ^{18}F-FDG, namely 4.38E-02 mGy/MBq and 4.04E-02 mGy/MBq, respectively, at the 8th week of gestation. For the fetus above 10 weeks of gestation, the bone marrow, brain, and thyroid receive the highest absorbed radiation doses from ^{18}F-FDG than other fetal tissues. The absorbed doses to the fetal bone marrow and thyroid from ^{18}F-FDG are about 35.1 % and 22.4 % higher than the average absorbed dose of fetal total body at 10–38 weeks of pregnancy. Figure 7 compares the S-values and absorbed dose per unit administered activity from I-124 for fetal thyroid between the values of this work and those reported in Watson [31]. The discrepancies between fetal thyroid S-values in these two works can be attributed to Johnson's radiation transport model for photons [32] used by Watson [31], which clearly results in underestimation of these values. In addition, differences between residence times used in the two works might result in additional discrepancies between absorbed dose estimates. Table 1 compares the estimated radiation doses per unit administered activity to the fetal total body for ^{18}F-FDG between this work and results reported in the literature. The absorbed doses from ^{18}F-FDG to the fetal total body in this work are 3.02E-02, 2.52E-02, 2.12E-02, 1.73E-02, 1.60E-02, 1.47E-02, 1.40E-02, and 1.32E-02 mGy/MBq at the 8th, 10th, 15th, 20th, 25th, 30th, 35th, and 38th week of pregnancy, respectively. The fetal absorbed doses obtained in this work are higher than those reported by Stabin et al. [14] at early pregnancy and at the 3rd month of gestation, but lower than the corresponding values for the fetus at 6 and 9 months of gestation. For the 3 months pregnant female phantom, the fetal mass in the work of Stabin et al. is 458 g while the ICRP suggested a value of 85 g. This might result in an underestimation of the fetal absorbed dose.

The effective dose provides a single number for estimating the radiobiological detriment from radiation exposure and allows comparisons of radiation risks associated with different imaging techniques/scenarios. However, the effective dose of the fetus has never been reported in the literature. In this work, the

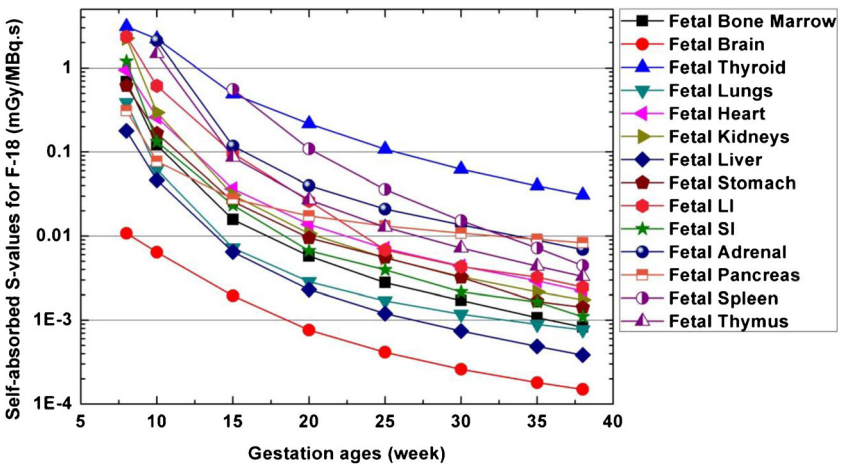

Fig. 3 Self-absorbed S-values to representative fetal organs from F-18

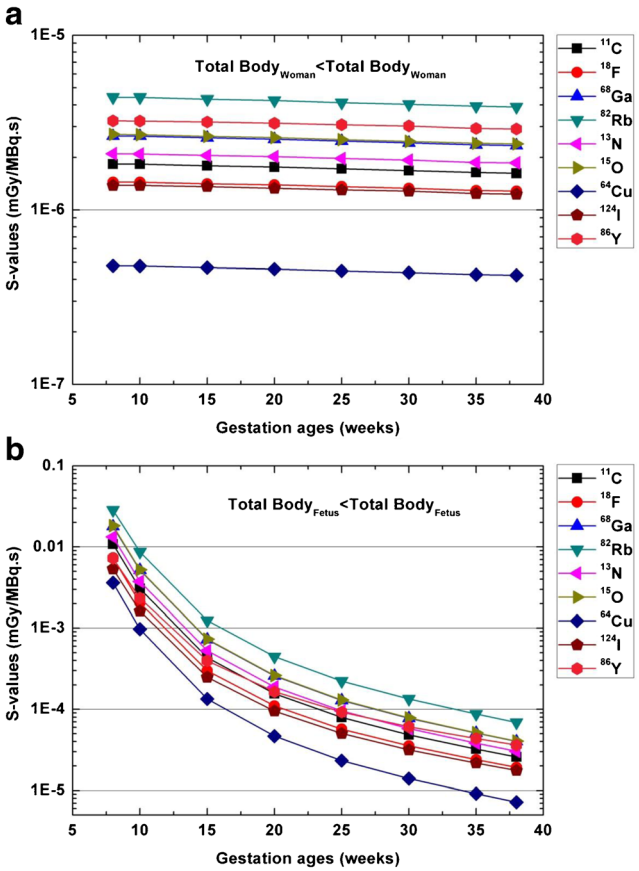

Fig. 4 Self-absorbed S-values for various radionuclides for (**a**) maternal total body and (**b**) fetal total body

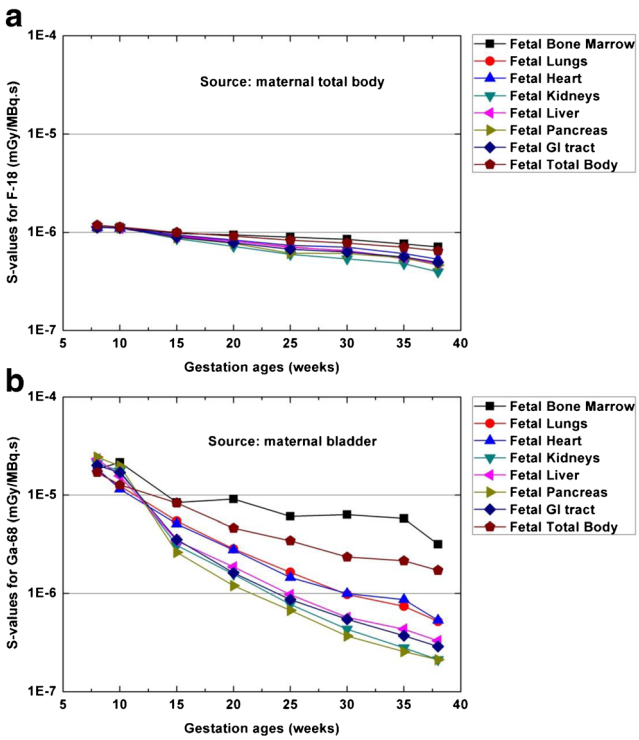

Fig. 5 Cross-absorbed S-values for (**a**) maternal body and (**b**) maternal bladder irradiating representative fetal organs

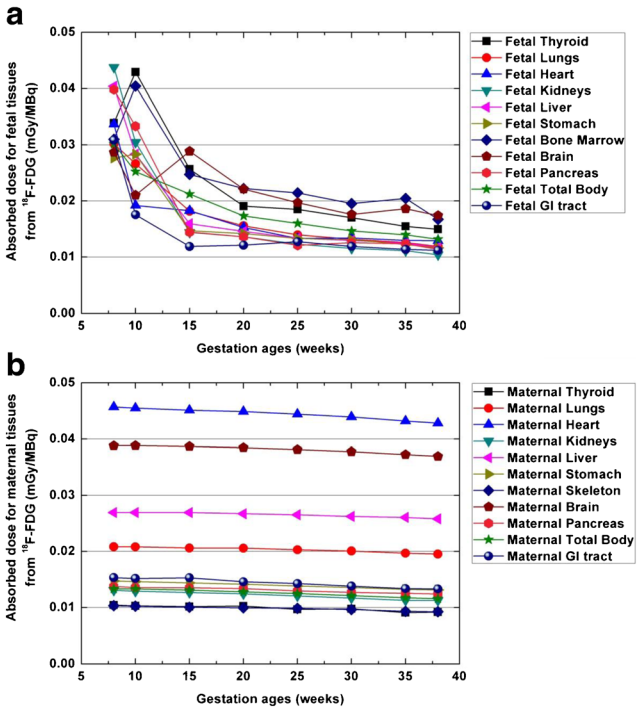

Fig. 6 Absorbed dose per unit administered activity from ^{18}F-FDG for (**a**) fetal tissues and (**b**) maternal tissues

effective dose of the fetus was calculated at various gestations from common positron-emitting radiotracers (Table 2). Since ^{18}F-FDG, ^{18}F-FDOPA, ^{11}C-labeled metahydroxephedrine and ^{68}Ga-DOTANOC are commonly used for PET imaging of pheochromocytoma in pregnant patients, we observed that ^{18}F-FDOPA produces the highest fetal effective dose. Figure 8 compares the effective doses of the fetus and pregnant women from ^{18}F-FDG and ^{68}Ga-DOTANOC. For the pregnant female, the effective dose changes slightly during the whole gestation period while the fetal effective doses are significantly higher at the 8th and 10th weeks of pregnancy than the other gestation periods. For ^{18}F-FDG, the fetal effective doses at the 8th and 10th weeks of pregnancy are 2.28 and 2.42 times larger than those of the 38th week of pregnancy. The fetal effective dose at the 10th week of pregnancy is higher than at the 8th week of pregnancy because more critical organs are considered in the phantom at the10th week of pregnancy.

Fetal dose from ^{18}F-FDG in clinical scans

Table 3 compares the fetal dose in the new series of pregnant female phantoms with those reported in the literature. Patient#1 (5th week pregnancy) receives the highest absorbed dose (9.69 mGy) from ^{18}F-FDG. The fetal doses estimated in this work are 1.1–2.1 times higher than the corresponding reported values. For early pregnancy (5–15 weeks of pregnancy), the recalculated fetal dose is about 28.1 % higher than those reported by Zanotti-Fregonara et al. [12]. For the fetus at the 8th week of pregnancy (patient#1), the cross-absorbed

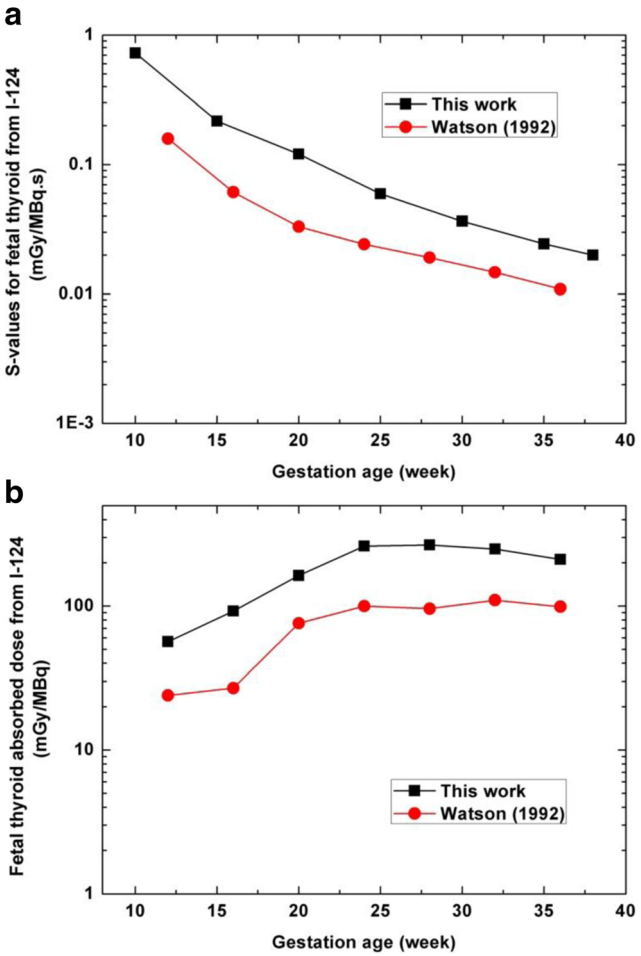

Fig. 7 Comparison of (**a**) S-values and (**b**) absorbed doses per unit administered activity from I-124 for fetal thyroid between the values of this work and Watson (1992)

dose from the maternal body and the self-absorbed dose from fetal body contributed 70 % and 26 % of the total fetal dose, respectively, while the uterine, placenta, amniotic fluid, and vesicle Vitelline contributed 4 % of the fetal dose in total. For the fetus at the 30th week of pregnancy (patient#10), the cross-absorbed dose from the maternal body and the self-absorbed dose from the fetal body contributed 36 % and 47 % of the total fetal dose, respectively, while the uterine, placenta, amniotic fluid, and umbilical cord contributed 17 % of the fetal dose in total. For ^{18}F-FDG in pregnant patients, the component of fetal absorbed dose from maternal body decreases with gestational age while the self-absorbed dose of the fetus increases with gestational age.

Discussion

The new generation of pregnant female phantom series constructed in this work is based on advanced boundary representation geometries in the form of NURBS and polygonal meshes, which combine both the flexibility of the simplified mathematical equations of mathematical models and the anatomic realism of voxel-based models. This modeling enables the generation of new phantoms by exploiting the flexibility offered for altering body contour shapes and the ability of repositioning the embedded fetus within the maternal uterus. The masses of tissues and organs of the developed computational fetal/pregnant female phantoms fit well with the corresponding reference values recommended by the ICRP for most organs and tissues, except in a few cases as mentioned above. S-values of nine positron-emitting radionuclides were calculated for the fetus and maternal body at eight gestation periods. Both the self-absorbed S-values for the fetal total body and the cross-absorbed S-values for the maternal body irradiating the fetus decrease with gestational age. For F-18, the dependence of

Table 1 Comparison of fetal absorbed dose from ^{18}F-FDG in pregnant female at different gestation periods

Radiotracer: ^{18}F-FDG	Fetal absorbed dose at different gestation periods (mGy/MBq)							
	8 weeks	10 weeks	15 weeks	20 weeks	25 weeks	30 weeks	35 weeks	38 weeks
Russell et al. [9]	2.70E-02 (Early Pregnancy)	1.7E-02 (12 weeks)	-	-	9.40E-03 (24 weeks)	-	8.10E-03 (36 weeks)	-
Stabin [14]	2.20E-02 (Early Pregnancy)	2.2E-02 (12 weeks)	-	-	1.70E-02 (24 weeks)	-	1.70E-02 (36 weeks)	-
Zanotti-Fregonara et al. [11]	-	4.00E-02	-	-	-	-	-	-
Zanotti-Fregonara et al. [10]	3.30E-02 (8 weeks)	-	-	-	-	-	-	-
Takalkar et al. [13]	1.55E-02 (6 weeks)	-	-	7.16E-03 (18 weeks)	6.23E-03	1.06E-02	-	-
Xie et al. [15]	3.05E-02 (Early Pregnancy)	2.27E-02 (12 weeks)	-	-	1.50E-02 (24 weeks)	-	1.33E-02 (36 weeks)	-
Zanotti-Fregonara et al.[12]	2.46E-02 (5 weeks)	1.31E-02 (12 weeks)	-	6.78E-02 (19 weeks)	-	8.26E-03 (28 weeks)	-	-
This work	3.02E-02	2.52E-02	2.12E-02	1.73E-02	1.60E-02	1.47E-02	1.40E-02	1.32E-02

Table 2 Comparison of fetal effective doses from investigated radiotracers in pregnant female at different gestation periods

Radiotracers	Fetal effective dose at different gestation periods (mSv/MBq)							
	8 weeks	10 weeks	15 weeks	20 weeks	25 weeks	30 weeks	35 weeks	38 weeks
^{11}C-acetate	2.46E-03	2.27E-03	2.10E-03	2.13E-03	2.15E-03	2.06E-03	2.05E-03	1.98E-03
^{11}C-amino acids	5.55E-03	4.94E-03	3.84E-03	3.65E-03	3.59E-03	3.38E-03	3.35E-03	3.18E-03
^{11}C brain receptor substances	7.49E-03	6.64E-03	4.22E-03	3.81E-03	3.62E-03	3.39E-03	3.34E-03	3.12E-03
^{11}C-methionine	1.29E-02	1.16E-02	5.41E-03	4.38E-03	3.77E-03	3.47E-03	3.38E-03	3.04E-03
^{11}C (realistic maximum model)	2.22E-02	1.98E-02	8.03E-03	6.01E-03	4.82E-03	4.34E-03	4.15E-03	3.58E-03
[Methyl-^{11}C]thymidine	3.30E-03	3.02E-03	2.81E-03	2.85E-03	2.89E-03	2.78E-03	2.79E-03	2.71E-03
^{11}C-thymidine	3.37E-03	2.93E-03	2.63E-03	2.60E-03	2.61E-03	2.48E-03	2.46E-03	2.36E-03
^{11}C-SA4503	3.77E-03	3.49E-03	3.19E-03	3.15E-03	3.17E-03	3.01E-03	3.03E-03	2.92E-03
^{11}C-MPDX	4.50E-03	4.01E-03	3.52E-03	3.41E-03	3.41E-03	3.23E-03	3.21E-03	3.07E-03
^{11}C-TMSX	4.46E-03	3.96E-03	3.48E-03	3.41E-03	3.42E-03	3.25E-03	3.23E-03	3.09E-03
^{11}C-CHIBA-1001	4.42E-03	4.30E-03	3.89E-03	3.55E-03	3.45E-03	3.15E-03	3.20E-03	3.05E-03
^{11}C-4DST	5.75E-03	5.13E-03	3.80E-03	3.61E-03	3.53E-03	3.35E-03	3.31E-03	3.15E-03
^{15}O-water	4.75E-04	5.38E-04	4.73E-04	4.78E-04	4.67E-04	4.40E-04	4.38E-04	4.23E-04
^{18}F-amino acids	2.15E-02	2.52E-02	1.69E-02	1.57E-02	1.49E-02	1.43E-02	1.40E-02	1.31E-02
^{18}F brain receptor substances	2.54E-02	2.81E-02	1.73E-02	1.59E-02	1.50E-02	1.43E-02	1.41E-02	1.32E-02
^{18}F-FDG	2.90E-02	3.09E-02	1.79E-02	1.59E-02	1.47E-02	1.40E-02	1.37E-02	1.27E-02
^{18}F-L-DOPA	5.06E-02	4.84E-02	2.26E-02	1.85E-02	1.57E-02	1.46E-02	1.40E-02	1.25E-02
^{18}F-FBPA	4.01E-02	4.28E-02	2.20E-02	1.88E-02	1.68E-02	1.59E-02	1.53E-02	1.41E-02
^{18}F-FDOPA	5.52E-02	5.40E-02	2.61E-02	2.16E-02	1.86E-02	1.73E-02	1.66E-02	1.49E-02
^{68}Ga-EDTA	4.43E-02	4.57E-02	2.23E-02	1.90E-02	1.68E-02	1.57E-02	1.50E-02	1.38E-02
^{68}Ga-DOTANOC	1.71E-02	1.93E-02	1.31E-02	1.25E-02	1.18E-02	1.13E-02	1.10E-02	1.05E-02

the self-absorbed S-value of fetal total body on gestational age are given by:

$$S_{Fetal\ Body}^{Fetus \rightarrow Fetus} = 79.61 \times (GW)^{-4.483} \quad (1)$$

whereas the dependence of fetal total body on the cross-absorbed S-value on gestational age can be given as:

$$S_{Fetal\ Body}^{Maternal\ Body \rightarrow Fetus} = -1.697 \times 10^{-8} \times (GW) + 1.284 \times 10^{-6} \quad (2)$$

where *GW* is the gestation period of fetus (in weeks), varying from 8 to 38 weeks. These rules can be used for a quick and rough estimation of the fetal total body absorbed dose from F-18 labeled radiotracers:

$$D_{Fetal\ Body} = MRT_{Maternal\ Body} \times S_{Fetal\ Body}^{Maternal\ Body \rightarrow Fetus} + MRT_{Fetus} \times S_{Fetal\ Body}^{Fetus \rightarrow Fetus} \quad (3)$$

where *D* is the absorbed dose in mGy/MBq and MRT is the mean residence time or time-integrated activity (MBq.s/MBq) of F-18 labeled tracers in the maternal total body or the fetus.

The absorbed and effective doses from 21 positron-emitting labeled radiotracers were estimated for 25 fetal tissues and the fetal total body. In this work, the standard MIRD formalism was adopted for estimating radiation doses to each organ. However, some molecules are designed to be delivered specifically to the blood vessels for diagnostic and/or therapeutic applications. As such, the mean residence time of these radiotracers in the blood would be higher than the MIRD estimates, thus resulting in higher absorbed dose to the endothelial walls, especially for small vessels.

For radiation dosimetry of radiotracers based on anthropomorphic computational phantoms, the effective dose presents a lower uncertainty compared to absorbed doses derived from clinical data [33]. However, the published literature indicates that the absorbed dose of the fetal total body from radiotracers is frequently considered while the fetal effective dose is rarely reported. The effective dose of the fetus estimated in this work can be used for comparison of the risks associated with different diagnostic imaging techniques/scenarios in regard to the potential radiobiological detriment to various developing fetal tissues. The fetal effective doses at the 8th and 10th weeks of gestation are significantly higher than those at other gestation periods because of the significantly lower fetal weight at early pregnancy.

For ^{18}F-FDG, the difference of organ absorbed doses calculated from different mathematical and voxel-based phantoms can be greater than 150 % [33]. We calculated fetal absorbed dose for a number of clinical studies reported in the literature based on reported time-integrated

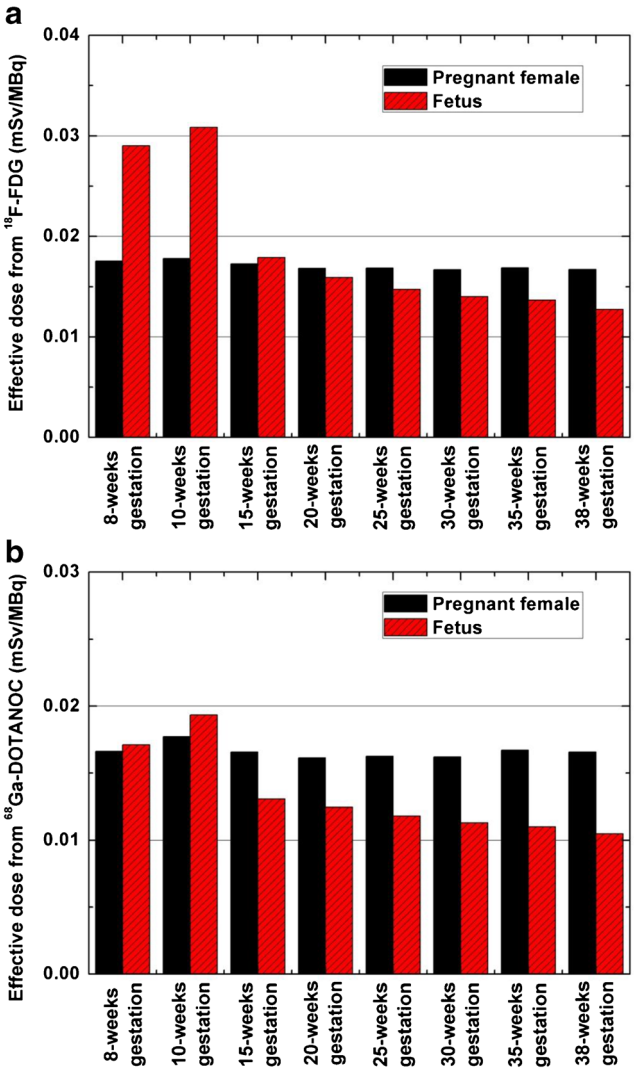

Fig. 8 Effective dose per unit administered activity for the fetus and pregnant female from (**a**) ^{18}F-FDG and (**b**) ^{68}Ga-DOTANOC

activity coefficients for the fetus and the developed anthropomorphic pregnant female phantoms. The fetal absorbed doses calculated in this work are about 10.3–110.3 % higher than the corresponding values reported in the literature. For early pregnancy, the dose to the uterus was used as a surrogate of the dose to the fetus the calculations performed by Zanotti-Fregonara et al. [12] and Takalkar et al. [13]. However, the reference fetal weight recommended by the ICRP for early pregnancy, i.e. the 8th week of gestation (4.7 g) is significantly lower than the mass of the adult female uterus (80 g). The replacement of the fetus with maternal uterus in radiation dose calculations at early pregnancy will result in underestimation of S-values for the fetal total body. In this context, the new pregnant female phantoms can provide more accurate fetal absorbed dose from radiopharmaceuticals at early pregnancy.

Conclusion

A new series of computational anthropomorphic pregnant female phantoms for representing reference fetus and adult female at various gestation periods were constructed. The developed computational phantoms were used to conduct a systematic study for evaluation of radiation dose to the fetus and gravida from common positron-emitting radionuclides and radiotracers based on updated tissue weighting factors and biodistribution data. The latest generation computational models can provide more accurate radiation dose estimates for the growing fetus. The produced S-values can be used for assessment of radiation dose to pregnant patients and the fetus at different gestational ages from various positron-emitting radiotracers. The calculated dosimetric database can be exploited

Table 3 Comparison of fetal absorbed doses from ^{18}F-FDG for the reported pregnant patients

Patient no.	Stage of gestation (weeks)	Administered activity (MBq)	Fetal absorbed dose from ^{18}F-FDG			
			Values reported in literatures		This work	
			Dose to fetus (mGy/MBq)	Total dose to fetus (mGy)	Dose to fetus (mGy/MBq)	Total dose to fetus (mGy)
1[a]	5	296	2.46E-02	7.28	3.27E-02	9.69
2[a]	12	385	1.31E-02	5.04	1.62E-02	6.25
3[a]	12	350	1.36E-02	4.76	1.73E-02	6.06
4[a]	19	296	6.78E-03	2.01	1.43E-02	4.22
5[a]	19	348	6.29E-03	2.19	1.29E-02	4.50
6[a]	28	296	8.26E-03	2.44	1.38E-02	4.08
7[b]	18	200	1.03E-02	2.06	1.14E-02	2.27
8[b]	25	337	7.41E-03	2.50	1.33E-02	4.49
9[b]	28	174	6.93E-03	1.21	9.70E-03	1.69
10[b]	30	229	1.17E-02	2.68	1.38E-02	3.17
11[b]	23	181	7.27E-03	1.32	1.30E-02	2.35

[a] Patients reported by Zanotti-Fregonara et al. [12]

[b] Patients reported by Takalkar et al. [13]

for evaluation and comparison of radiation risks to pregnant patients and unborn embryo/fetus associated with different imaging techniques/scenarios. The fetal organ-level dose is rarely reported in literature. As the radio-sensitivity and radiation risks of developing fetal organs vary across different trimesters, the estimation of organ-level radiation dose to the fetus may pave the way for a detailed investigation of the correlations between radiation exposure of the uterus and organ-specific childhood cancer after birth. The developed fetus models and pregnant female phantoms matching the ICRP reference data can be used for calculation of internal/external radiation absorbed dose to provide standardized dose estimates for various radiotracers in clinical and research settings.

Acknowledgments This work was supported by the Swiss National Science Foundation under Grant SNSF 31003A-149957. The authors would like to thank Prof. George Xu (Rensselaer Polytechnic Institute, New York), Dr Isabelle Bloch (Telecom ParisTech) and Dr Maria Zankl (Helmholtz Zentrum München) for providing the pregnant and fetal computational models.

Compliance with ethical standards 1. Disclosure of potential conflicts of interest: none of the authors have affiliations that present financial or non-financial competing interests for this work.

2. Research involving human participants: All procedures performed in studies involving human participants were in accordance with the ethical standards of the institutional and/or national research committee and with the 1964 Helsinki declaration and its later amendments or comparable ethical standards.

3. Informed consent: informed consent was obtained from all individual participants included in the study.

Conflict of Interest The authors declare that they have no conflict of interest.

References

1. Gambhir SS. Molecular imaging of cancer with positron emission tomography. Nat Rev Cancer. 2002;2:683–93.
2. Xie T, Bolch WE, Lee C, Zaidi H. Pediatric radiation dosimetry for positron-emitting radionuclides using anthropomorphic phantoms. Med Phys. 2013;40:102502–14.
3. Xie T, Zaidi H. Evaluation of radiation dose to anthropomorphic paediatric models from positron-emitting labelled tracers. Phys Med Biol. 2014;59:1165–87.
4. Kusama T, Ota K. Radiological protection for diagnostic examination of pregnant women. Congenit Anom (Kyoto). 2002;42:10–4.
5. Stabin MG. Radiation dose concerns for the pregnant or lactating patient. Semin Nucl Med. 2014;44:479–88.
6. Altman KI, Lett JT. Relative radiation sensitivities of human organ systems: Vol. 15, Elsevier; 2013.
7. Zaidi H, Xu XG. Computational anthropomorphic models of the human anatomy: The path to realistic Monte Carlo modeling in medical imaging. Annu Rev Biomed Eng. 2007;9:471–500.
8. Stabin MG, Watson E, Cristy M, Ryman J, Eckerman K, Davis J, et al. Mathematical models and specific absorbed fractions of photon energy in the nonpregnant adult female and at the end of each trimester of pregnancy. Oak Ridge National Lab., TN (United States); 1995.
9. Russell JR, Stabin MG, Sparks RB, Watson E. Radiation absorbed dose to the embryo/fetus from radiopharmaceuticals. Health Phys. 1997;73:756–69.
10. Zanotti-Fregonara P, Jan S, Champion C, Trébossen R, Maroy R, Devaux J-Y, et al. In vivo quantification of 18F-FDG uptake in human placenta during early pregnancy. Health Phys. 2009;97:82–5.
11. Zanotti-Fregonara P, Jan S, Taieb D, Cammilleri S, Trébossen R, Hindié E, et al. Absorbed 18F-FDG dose to the fetus during early pregnancy. J Nucl Med. 2010;51:803–05.
12. Zanotti-Fregonara P, Laforest R, Wallis JW. Fetal radiation dose from 18F-FDG in pregnant patients imaged with PET, PET/CT, and PET/MR. J Nucl Med. 2015;56:1218–22.
13. Takalkar AM, Khandelwal A, Lokitz S, Lilien DL, Stabin MG. 18F-FDG PET in pregnancy and fetal radiation dose estimates. J Nucl Med. 2011;52:1035–40.
14. Stabin MG. Proposed addendum to previously published fetal dose estimate tables for 18F-FDG. J Nucl Med. 2004;45:634–35.
15. Xie T, Zaidi H. Fetal and maternal absorbed dose estimates for positron-emitting molecular imaging probes. J Nucl Med. 2014;55:1459–66.
16. ICRP. Publication 89: Basic anatomical and physiological data for use in radiological protection: reference values. Ann ICRP. 2002;32:1–277.
17. Xu XG, Taranenko V, Zhang J, Shi C. A boundary-representation method for designing whole-body radiation dosimetry models: pregnant females at the ends of three gestational periods—RPI-P3, −P6 and -P9. Phys Med Biol. 2007;52:7023–44.
18. Bibin L, Anquez J, de la Plata Alcalde JP, Boubekeur T, Angelini ED, Bloch I. Whole-body pregnant woman modeling by digital geometry processing with detailed uterofetal unit based on medical images. IEEE Trans Biomed Eng. 2010;57:2346–58.
19. Becker J, Zankl M, Fill U, Hoeschen C. Katja—the 24th week of virtual pregnancy for dosimetric calculations. Pol J Med Phys Eng. 2008;14:13–20.
20. Petoussi-Henss N, Zankl M, Fill U, Regulla D. The GSF family of voxel phantoms. Phys Med Biol. 2002;47:89.
21. Xie T, Zaidi H. Construction of pregnant female phantoms at different gestation periods for radiation dosimetry. Proc of the 5th International Workshop on Computational Phantoms for Radiation Protection, Imaging and Radiotherapy. Seoul, Korea, 19–22 July 2015; 2015; p. 4–5.
22. Patrick M. Binvox code - 3D mesh voxelizer. Princeton University: Princeton University.
23. Pelowitz DB. MCNPX User's Manual Version 2.5.0. Los Alamos National Laboratory: Los Alamos, NM; 2005.
24. ICRP. ICRP publication 80: Radiation dose to patients from radiopharmaceuticals (addendum 2 to ICRP publication 53). Ann ICRP. 1998;28:1–126.
25. ICRP. ICRP Publication 106: Radiation dose to patients from radiopharmaceuticals. Addendum 3 to ICRP Publication 53. Ann ICRP. 2008;38:1–197.
26. Sakata M, Oda K, Toyohara J, Ishii K, Nariai T, Ishiwata K. Direct comparison of radiation dosimetry of six PET tracers using human whole-body imaging and murine biodistribution studies. Ann Nucl Med. 2013;27:285–96.
27. Pettinato C, Sarnelli A, Di Donna M, Civollani S, Nanni C, Montini G, et al. 68Ga-DOTANOC: biodistribution and dosimetry in patients affected by neuroendocrine tumors. Eur J Nucl Med Mol Imaging. 2008;35:72–9.
28. Bolch WE, Eckerman KF, Sgouros G, Thomas SR. MIRD Pamphlet No. 21: A generalized schema for radiopharmaceutical dosimetry - Standardization of nomenclature. J Nucl Med. 2009;50:477–84.

29. ICRP. ICRP Publication 103: The 2007 Recommendations of the International Commission on Radiological Protection. Ann ICRP. 2007;37:1–332.
30. Benveniste H, Fowler JS, Rooney WD, Moller DH, Backus WW, Warner DA, et al. Maternal-fetal in vivo imaging: a combined PET and MRI study. J Nucl Med. 2003;44:1522–30.
31. Watson E. Radiation absorbed dose to the human fetal thyroid. Proc. Fifth International Radiopharmaceutical Dosimetry Symposium: Oak Ridge Associated Universities Oak Ridge, TN; 1992; p. 179–87.
32. Johnson J. Fetal thyroid dose from intakes of radioiodine by the mother. Health Phys. 1982;43:573–82.
33. Spielmann V, Li WB, Zankl M, Oeh U, Hoeschen C. Uncertainty quantification in internal dose calculations for seven selected radiopharmaceuticals. J Nucl Med. 2016;57:122–28.